Transcriptional control of O -methylguanine DNA methyltransferase expression and temozolomide resistance in glioblastoma

Happold, Caroline ; Stojcheva, Nina ; Silginer, Manuela ; Weiss, Tobias ; Roth, Patrick ; Reifenberger, Guido ; Weller, Michael

Abstract: O -methylguanine DNA methyltransferase (MGMT) promoter methylation is a predictive biomarker for benefit from alkylating chemotherapy, specifically temozolomide (TMZ), in glioblastoma, the most common malignant intrinsic brain tumor. Glioma-initiating cells (GIC) with stem-like properties have been associated with resistance to therapy and progression. We assessed the levels of MGMT mRNA and MGMT protein by real-time PCR and immunoblot and evaluated the impact of MGMT on TMZ sensitivity in clonogenicity assays in GIC sphere cultures (S) or differentiated adherent monolayer cultures (M). Nuclear factor kappa B (NF- B) signaling was assessed by reporter assay and immunoblot. Compared to M cells, S cells expressed higher levels of MGMT. Differentiation of GIC induced by S-to-M transition resulted in a gradual loss of MGMT expression and increased TMZ sensitivity. This transcriptional regulation of MGMT was restricted to cell lines without MGMT promoter methylation and was not coupled to any specific neurobasal (NB) stem cell medium supplement or loss of cell adhesion. Expression levels of p50/p65 subunits of NF- B, a transcriptional regulator of MGMT, were increased in S cells. Inhibition of NF- B by the small molecule inhibitor, BAY 11-7082, or siRNA-mediated gene silencing, reduced MGMT levels. In summary, alkylator resistance of S cells is mainly promoted by over-expression of MGMT which results from increased activity of the NF- B pathway in this cell culture model of glioma stem-like cells. Read the Editorial Highlight for this article on page 688.

DOI: https://doi.org/10.1111/jnc.14326

Transcriptional control of O^6-methylguanine DNA methyltransferase expression and temozolomide resistance in glioblastoma

Caroline Happold[1], Nina Stojcheva[1], Manuela Silginer[1], Tobias Weiss[1], Patrick Roth[1], Guido Reifenberger[2], Michael Weller[1]

[1]Laboratory of Molecular Neuro-Oncology, Department of Neurology, University Hospital and University of Zurich, Zurich, Frauenklinikstrasse 26, and Neuroscience Center Zurich, University of Zurich, 8091 Zurich, Switzerland; [2]Department of Neuropathology, Heinrich-Heine-University Düsseldorf, Düsseldorf, and German Cancer Consortium (DKTK), partner site Essen/Düsseldorf, Germany

*Correspondence: Dr. Caroline Happold, Department of Neurology, University Hospital Zurich, Frauenklinikstrasse 26, 8091 Zurich, Switzerland, Tel.: +41 (0)44 255 3087, Fax: +41 (0)44 255 4380, E-mail: caroline.happold@usz.ch

Funding: Supported by a grant from the Wilhelm Sander Foundation for Cancer Research to MW and GR (2012.088.1).

Total word count: 4,200 + 922 legends words w/o references (abstract 220)

Running title: MGMT expression in glioma stem-like cells

Keywords: MGMT, glioma stem cell, temozolomide, therapy resistance, NF-κB

Abstract *(max.250w)*

O^6-methylguanine DNA methyltransferase (*MGMT*) promoter methylation is a predictive biomarker for benefit from alkylating chemotherapy, specifically temozolomide (TMZ), in glioblastoma, the most common malignant intrinsic brain tumor. Glioma-initiating cells (GIC) with stem-like properties have been associated with resistance to therapy and progression. We assessed the levels of *MGMT* mRNA and MGMT protein by real-time PCR and immunoblot and evaluated the impact of MGMT on TMZ sensitivity in clonogenicity assays in GIC sphere cultures (S) or differentiated adherent monolayer cultures (M). ~~Similar experiments were performed in long-term glioma cell lines (LTC)~~. Nuclear factor kappa B (NF-κB) signalling was assessed by reporter assay and immunoblot. Compared to M cells, S cells expressed higher levels of MGMT. Differentiation of GIC induced by S-to-M transition resulted in a gradual loss of MGMT expression and increased TMZ sensitivity. This transcriptional regulation of *MGMT* was restricted to cell lines without *MGMT* promoter methylation and was not coupled to any specific neurobasal (NB) stem cell medium supplement or loss of cell adhesion. Expression levels of p50/p65 subunits of NF-κB, a transcriptional regulator of *MGMT*, were increased in S cells. Inhibition of NF-κB by the small molecule inhibitor, BAY 11-7082, or siRNA-mediated gene silencing, reduced MGMT levels. In summary, alkylator resistance of S cells is mainly promoted by overexpression of MGMT which results from increased activity of the NF-κB pathway in this cell culture model of glioma stem-like cells.

Abbreviations

BMP-4, bone morphogenetic protein-4; CAIX, carbonic anhydrase 9; CIL, cilengitide; DMEM, Dulbecco`s modified Eagle medium; FGF, fibroblast growth factor; FCS, fetal

calf serum; GAL, GLPG0187; GAPDH, glyceraldehyde-3-phosphate dehydrogenase; GIC, glioma-initiating cell; ITGA6, Integrin alpha-6 precursor; ITGB1, Integrin beta-1 precursor; KPS, Karnofsky performance score; L1CAM, neural cell adhesion molecule L1; LTC, long-term cell line; M, monolayer cells or cultures; MGMT, O^6-methylguanine DNA methyltransferase; NANOG, homeobox protein nanog; NB, neurobasal medium; NF-κB, nuclear factor kappa B; OCT4, octamer binding transcription factor 4; PBS, phosphate-buffered saline; qPCR, quantitative polymerase chain reaction; RAD, cyclo-(Arg-Ala-Asp-DPhe-Val); RRID, Research Resource Identifiers; S, sphere cells or cultures; TMZ, temozolomide.

Introduction

Glioblastomas, the most malignant primary brain tumors in adults, are characterized by their infiltrative growth pattern and resistance to radiotherapy and cytotoxic chemotherapy. Current multimodality treatment approaches include surgery, radiotherapy and alkylating agent chemotherapy using temozolomide (TMZ) (Weller *et al.* 2017); yet, recurrence is inevitable and median survival is still in the range of 12-17 months (Johnson & O'Neill 2012, Gramatzki *et al.* 2016). Tumors lacking methylation of the promoter region of the O^6-methylguanine-DNA-methyltransferase (*MGMT*) gene, which encodes a DNA repair protein, are especially prone to early progression during standard chemoradiotherapy (Hegi *et al.* 2005).

Glioma-initiating cells (GIC), also referred to as stem-like glioma cells, are a subpopulation of cells within a glioma considered to maintain a pool of highly treatment-resistant cells responsible for treatment failure and progression (Lathia *et al.* 2015). The role of MGMT specifically in the GIC compartment has been addressed in various experimental approaches, but no uniform concept has emerged (Beier *et al.* 2008, Blough *et al.* 2010, Sciuscio *et al.* 2011). In a panel of ten paired samples of glioblastomas and their derived sphere cultures, *MGMT* promoter methylation was highly enriched in sphere cells, with MGMT protein levels being accordingly reduced (Sciuscio et al. 2011). Glioma-derived stem cells with sphere forming capacity have even been suggested as preferential targets of TMZ-induced tumor cell depletion (Beier et al. 2008). Other groups have shown a heterogeneous pattern of resistance to TMZ in GIC cultures, with resistant as well as sensitive GIC displaying heterogeneous *MGMT* promoter methylation, concluding that its mere presence does not predict sensitivity to TMZ. Yet, MGMT protein levels correlated with TMZ sensitivity in this panel of 20 GIC (Blough et al. 2010). In cultures of side population-derived neurospheres, stem cell properties and MGMT expression were enriched compared to the bulk population of tumor cells (Bleau *et al.* 2009). Yet,

more recently the side population has been proposed to consist essentially of non-neoplastic cells (Golebiewska *et al.* 2013) which would explain increased MGMT expression. Here we explore the relationship between the stemness phenotype of cultured glioma cells and MGMT expression *in vitro* and link nuclear factor kappa B (NF-kB) activation with consecutive MGMT induction to stemness and chemoresistance.

Materials and Methods

Reagents

TMZ was provided by Schering-Plough (Kenilworth, NJ). A stock solution of TMZ at 200 mM was prepared in dimethylsulfoxide (DMSO) and stored at -20°C. Human MGMT antibody was purchased from Alpha Diagnostics *(*San Antonio, TX). Glyceraldehyde-3-phosphate dehydrogenase (GAPDH) antibody (EB07069) (RRID:AB_2247304) was obtained from Everest Biotech (Oxfordshire, UK). β-Actin antibody (sc-1616) (RRID:AB_630836) was obtained from Santa Cruz Biotechnology (Dallas, TX). BAY 11-7082 (Selleckchem, Houston, TX) was prepared as 50 mM stock solution in DMSO. Cilengitide (EMD121974) was kindly provided by Merck KGaA (Darmstadt, Germany). GLPG0187 was kindly provided by Galapagos NV (Mechelen, Belgium). RAD peptide cyclo-Arg-Ala-Asp-DPhe-Val was purchased from Bachem AG (Bubendorf, Switzerland). Bone morphogenetic protein (BMP)-4 was from R&D (Minneapolis, MN). O^6-benzylguanine (O^6-BG) and all other reagents, unless indicated otherwise, were purchased from Sigma (St. Louis, MO).

Cell lines

The human glioma-initiating (stem-like) cell lines (GIC) GS-2, GS-5, GS-7, GS-8, GS-9 (Gunther *et al.* 2008), T-325 (Lemke *et al.* 2014), ZH-161 and ZH-305 (Silginer *et al.* 2016, Stojcheva *et al.* 2016) were maintained as sphere (S) cultures in Neurobasal Medium® supplemented with 2% B-27 supplement, 1% GlutaMAX, 20 ng/ml epidermal growth factor (EGF), 20 ng/ml fibroblast growth factor (FGF) and 32 IE/ml heparin. The human glioma cell line T98G (RRID:CVCL_0556**)** was purchased from the American Type Culture Collection (Rockville, MD). The glioma cell lines LN-18 (RRID:CVCL_0392) , LN-229 (RRID:CVCL_0393) and LN-308

(RRID:CVCL_0394) were kindly provided by N. de Tribolet (Lausanne, Switzerland). LN-18_R cells have been described (Happold *et al.* 2012). These long-term cell lines (LTC) were commonly cultured as monolayers (M) in Dulbecco's modified Eagle medium (DMEM) containing 10% FCS and 2 mM glutamine from Gibco Life Technologies (Carlsbad, CA). LN-229_MGMT and LN-229_Neo cells have been described (Hermisson *et al.* 2006). In selected experiments the culture conditions were switched for both GIC and LTC, as outlined below. Cells isolated from freshly resected human glioblastoma tumor tissue (ZH-464, ZH-456, ZH-419, ZH-496 and ZH-525) were collected after written informed consent of the patients and approval by the institutional review board. Briefly, these cells were extracted from tumor tissue by dissociating tissue with 10 mg/ml collagenase/dispase (Roche, Basel, Switzerland) and gentle rotation in MACS C-tubes (Miltenyi biotech, Cologne, Germany). Cells were counted and 20 µl of FcR blocking reagent and 20 µl of CD133 microbeads (Miltenyi biotech) were added per 10^7 cells. Cells were incubated for 45 min at 4°C, passed through a 40 µm cell strainer, and then passed through an LS column placed in the magnetic field of the MACS separator. The passing CD133-negative population was passed a second time through a second column to get a purer CD133-negative population. CD133-positive cells remained in the column and were collected separately by forceful washing.

Quantitative PCR

Total RNA was prepared using the NucleoSpin System (Macherey-Nagel AG, Oensingen SO, Switzerland) and transcribed into cDNA. For real-time (quantitative) qPCR, cDNA amplification was monitored using SYBRGreen chemistry on the 7300 Real time PCR System (Applied Biosystems, Zug, Switzerland). The conditions were: 40 cycles, 95°C/15 sec, 60°C/1 min. Data analysis was done using the $\Delta\Delta C_T$ method

for relative quantification. The following specific primers were used: *GAPDH* fwd: 5'-CTCTCTGCTCCTCCTGTTCGAC-3', *GAPDH* rv: 5'-TGAGCGATGTGGCTCGGCT-3'; *MGMT* fwd: 5'-GTC GTT CAC CAG ACA GGT GTT A-3'; *MGMT* rv: 5'- ACA GGA TTG CCT CTC ATT GCT C-3'. *CD133* fwd: 5'-TGGATGCAGAACTTGACAACGT-3'; *CD133* rv: 5'-ATACCTGCTACGACAGTCGTGGT-3'; *GFAP* fwd: 5'-TCTCTCGGAGTATCTGGGAACTG-3'; *GFAP* rv: 5'-TTCCCTTTCCTGTCTGAGTCTCA-3'; *OCT4* fwd: 5'-TCTCCCATGCATTCAAACTGAG-3'; *OCT4* rv: 5'-CCTTTGTGTTCCCAATTCCTTC-3'*; MUSASHI* fwd: 5'-CCAATGGGTACCACTGAAGC-3'; *MUSASHI* rv: 5'-ACTCGTGGTCCTCAGTCAGC-3'; TUBB3 fwd: 5'-GCAACTACGTGGGCGACT-3'; TUBB3 rev: 5'-CGAGGCACGTACTTGTGAGA-3'; OLIG2 fwd: 5'-AGCTCCTCAAATCGCATCC-3'; OLIG2 rv: 5'-ATAGTCGTCGCAGCTTTCG-3'. For single cell quantitative real-time PCR, human glioblastoma samples were dissociated with papain (Worthington, Lakewood, NJ) and leukocytes were depleted by anti-human CD45–conjugated microbeads (Miltenyi Biotec, Bergisch Gladbach, Germany) using MACS LD columns (Miltenyi Biotec). Single cell qPCR was performed at the Genomics Facility Basel, Switzerland. C1 System (Fludigim, San Francisco, CA) was used to prepare single-cells for mRNA isolation, cDNA synthesis and pre-amplification. BioMark HD system was used for RT-PCR analysis of the pre-amplification products (Papa *et al.* 2017). The following primers were used: *SOX-4* (forward 5'-GGTCTCTAGTTCTTGCACGCT-3', reverse 5'-CTGCAAGAAGGGAGCTGGTAA-3'); SOX-2 (forward 5'-CACACTGCCCCTCTCAC-3'; reverse 5'-TCCATGCTGTTTCTTACTCTCC-3'); *MUSASHI* (forward 5'-CCAATGGGTACCACTGAAGC -3', reverse 5'-ACTCGTGGTCCTCAGTCAGC -3'); *CD133* (forward 5'- TGGATGCAGAACTTGACAACGT -3', reverse 5'-ATACCTGCTACGACAGTCGTGGT-3'); OCT4 (forward 5'-

CGAGAAGGATGTGGTCCGAG-3', reverse 5'-TGTGCATAGTCGCTGCTTGA-3'); NANOG (forward 5'-GAAATACCTCAGCCTCCAGC-3', reverse 5'-GCGTCACACCATTGCTATTC-3'); Nestin (forward 5'-GGCTGCGGGCTACTGAAA-3', reverse 5'-CTGAGCGATCTGGCTCTGTAG-3'); ITGB1 (forward 5'-AGCCTGTTTACAAGGAGCTGAA-3', reverse 5'-CGCCTTCTGACAATTTGCCG-3'); L1CAM (forward 5'- CCCCAGGTCACTATCGGCTA -3', reverse 5'-GACTGCCCTCCCTCCAGTA -3'); ITGA6 (forward 5'-TCAACAAGGATGGGTGGCAA-3', reverse 5'-TCTGCCTTGCTGGTTCATGT-3')

Single-cell gene expression analysis correlation experiments

Single-cell gene expression analysis has been described (Stahlberg *et al.* 2013). Low quality cells that did not express the housekeeping genes *ARF-1* or *ARF-1* were discarded; 481 cells from 6 patients were included in the analyses. Cq values were converted to expression levels using the equation $Log_2Ex = C_{q\ LOD\ (Limit\ of\ Detection)} - Cq$ with a LOD C_q of 25 and data was transformed using asinh transformation. Pearson`s correlation coefficients were computed using the corrplot R package version 0.77 and Bonferroni correction was applied to adjust for multiple hypothesis testing. Scatterplots of significant correlations were plotted using the ggpubr R package version 0.1.2.

Spherogenicity and clonogenicity assays

S cells were seeded at 500 cells per well of 96-well plates in neurobasal (NB) medium, treated 24 h later as indicated, and consecutively maintained in NB medium. For adherent M cultures, clonogenic assays were performed by seeding 100 cells (LN-229) or 300 cells (all other LTC or M cells) per well in 96-well plates and allowed to adhere overnight. The cells were exposed to TMZ at the indicated concentrations

for 24 h in serum-free medium, followed by an observation period for 7-14 days in the same medium. In the experiments involving O^6-BG, the cells were pretreated with O^6-BG or DMSO control for 2 h prior to TMZ application. Cell density was assessed by MTT assay for S conditions and by crystal violet staining for M conditions. Representative studies confirmed that the data obtained like that correspond well to data based on actual counts of spheres or colonies.

Immunoblot analysis

Cells treated as indicated were lysed on ice in radioimmunoprecipitation assay (RIPA) lysis buffer (150 mM NaCl, 25 mM Tris-HCl, pH 7.5, 1% Nonidet P-40, 1% sodium deoxycholate, 0.1% SDS, 1 mM phenylmethylsulfonyl fluoride, 1 mM sodium fluoride, 1 mM sodium pyrophosphate, 1 mM sodium orthovanadate, 1 µg/ml leupeptin, 1 mM ethylene glycol-bis(β-aminoethyl ether)-N,N,N',N'-tetraacetic acid (EGTA) supplemented with 1x complete inhibitor mix (Roche Diagnostics, Grenzach-Wyhlen, Germany). Pre-cleared cell lysates, mixed and boiled with Laemmli buffer containing β-mercaptoethanol, were resolved by sodium dodecyl sulfate polyacrylamide gel electrophoresis (SDS-PAGE) and transferred to nitrocellulose membranes (GE Healthcare; Little Chalfont, Buckinghamshire, UK). After blocking in Tris-buffered saline containing 5% skim milk and 0.05% Tween 20, the blots were incubated overnight at 4°C with primary antibodies and 1 h at room temperature for secondary antibodies. Visualization of protein bands was done using horseradish peroxidase-coupled secondary antibodies (Santa Cruz Biotechnology, Dallas, TX) and enhanced chemiluminescence (Pierce / Thermo Fisher, Madison, WI).

Reporter assay

Cells were either transfected by electroporation directly (for S cells) or by Lipofectamine 2000 reagent 24 h after seeding to a 96-well plate with 20,000 cells/well) (for M cells), with 200 ng of pNF-κB -Luc plasmid containing a firefly luciferase gene designed to detect NF-κB signalling activity, together with 20 ng of the control renilla plasmid pRL-CMV (Hermisson & Weller 2003). GIC were seeded at a density of 50,000 cells/well in 96-well plates after transfection. Further treatment was performed 18 h later, and cells were lysed 6 h post-treatment and luciferase activity was measured.

Transient transfection

GIC were dissociated using Accutase cell detachment solution (PAA Laboratories, Pasching, Austria), and $2x10^6$ cells were transfected using the Neon Transfection System electroporation device and kit (Invitrogen, Life Technologies) with 100 nM specific or control. Hereafter, cells were allowed to recover for a day under neurobasal conditions, and seeded for either survival assays or protein lysate isolation as described above.

Proliferation assays

Cells were seeded at a density of $1x10^5$ cells/well in a 96-well plate with 6 well replicates per time point, and left to grow for the indicated time points. Analysis was done by MTT assay as described above, and normalized to baseline time point.

Flow cytometry

For cell cycle analysis, GIC and LTC were harvested, fixed and washed with PBS. Hereafter, RNA was digested with RNase A (Carl Roth AG, Karlsruhe, Germany), DNA stained with propidium iodide (PI) (50 ug/ml) and fluorescence was recorded

with BD FACSVerse flow cytometer (BD, Heidelberg, Germany). For AnnexinV/PI flow cytometry, cells were incubated with FITC-labeled AnxV-fluorescin isothiocyanate and PI for 20 min. Fluorescence was recorded in with a BD FACSVerse flow cytometer. PI-positive (necrotic) or AnxV-positive (apoptotic) cells or double positive were counted as dead.

Statistical analyses

Data are representative of experiments independently performed three times with similar results unless indicated otherwise with the exception of the freshly resected tumor tissue cell-based experiments. Viability and proliferation studies were performed using triplicate wells. Where indicated, analysis of significance was performed using the two-tailed Student's t-test. Correlation analysis was done by Spearman test. No randomization or blinding was performed in this study. Study was not pre-registered.

Results

Sphere cultures of GIC are more resistant to TMZ than adherent cultures

GIC are considered to promote treatment resistance in glioblastoma and to retain an expression signature related to stemness that is gradually lost when multi-lineage differentiation and adherent monolayer growth are induced by exposure to FCS-containing medium (Fig. 1A,B; Supplementary Fig 1A) (Günter et al. 2008, Happold et al. 2014) . However, we noted that merely shifting of GIC cells from S to M conditions was associated with greatly enhanced sensitivity to TMZ (Fig. 1C, D). The EC_{50} values were shifted up to 10-fold in all GIC except for T-325 and GS-9. In ZH-305, the effect was even reversed (Fig. 1E). Limiting dilution assays were performed to further characterize TMZ sensitivity of S cells to TMZ as function of cell density (Supplementary Fig. 1B). No major changes in cell cycle distribution or proliferation rate were seen between S and M cells (Fig. 1F,G). Moreover, AnxV/PI flow cytometry did not confirm relevant cell death after exposure to TMZ at clinically relevant concentrations (Supplementary Fig. 1C).

High MGMT expression confers TMZ resistance in S cultures

We next investigated whether the loss of resistance to TMZ induced by switching from S to M culture conditions was associated with changes in MGMT expression. While most M cultures exhibited only minor decreases in *MGMT* mRNA expression levels compared with S cultures (Fig. 2A), we found consistent reduction of MGMT protein levels in M cultures (Fig. 2B). GS-9 and ZH-305, which did not show decreased EC_{50} values when switched to M conditions, did not express MGMT either under S or M conditions. There was strong correlation between *MGMT* mRNA levels determined by qPCR and TMZ sensitivity defined by EC_{50} values in clonogenicity

assays (r=0.79, p=0.0003) (Fig. 2C). To confirm that the changes in *MGMT* levels are responsible for the sensitization to TMZ during the S→M transition, we pre-exposed the cells to the MGMT pseudosubstrate inhibitor, O^6-BG, for 2 h before TMZ exposure. Consumption of MGMT levels by O^6-BG within 72 h was verified by immunoblot analysis. Indeed, pre-exposure to O^6-BG shifted the sensitivity of S cultures to TMZ to the range of M cultures (for GS-2) or lower (for GS-5) in clonogenic survival assays (Fig. 2D).

MGMT expression correlates with expression of stemness markers

Single cell gene expression analysis performed from freshly resected glioma tissue confirmed positive correlation of *MGMT* with various stem cell markers, although not Musashi (Fig. 3A). Additionally, to confirm differential MGMT expression ex *vivo*, we investigated MGMT expression in isolated CD133-positive cells, considered stem-like, versus CD133-negative sorted cells, from freshly resected tumor tissues of five glioblastoma patients. *MGMT* mRNA levels were increased at least 2-fold in CD133+ cells in all patients (Fig. 3B). Conversely, induction of differentiation by bone morphogenetic protein(BMP)-4 decreased MGMT protein levels in 3 out of 4 S cell lines (Fig. 3C), as well as CD133 mRNA expression in 3 out of 4 cell lines except for a reversed effect in T-325, while increasing GFAP mRNA expression (Fig. 3D).

Impact of culture conditions on MGMT expression in glioma cells

To better understand the regulation of MGMT expression in S versus M cells, we studied the time course of MGMT loss upon S→M transition in more detail. The switch of GS-2 and GS-5 S to M conditions led to a rapid drop of MGMT levels in GS-5 (d1) and a delayed decline in GS-2 (d12) (Fig. 4A). Conversely, when the M cells were returned to S conditions, they formed spheres again and accumulated MGMT

protein, with GS-2 displaying earlier protein level changes (d1) than GS-5 (d5), indicating that this effect, albeit consistent, had variable time kinetics in different model systems (Fig. 4B). MGMT regulation was directly or indirectly linked to the additional components of the NB medium since cells maintained in NB medium only did not accumulate MGMT to the extent of cells maintained in NB medium plus supplements (Fig. 4C). Cell death because of lack of supplements was excluded as a cause for lower MGMT levels (Fig. 4D).

In order to assess whether a specific medium supplement was responsible for the regulation of MGMT expression in S cells, we starved GS-2 and GS-5 from individual medium supplements. We found that, while sphere formation and volume were reduced when growth factors were removed from the medium (data not shown), the levels of MGMT did not significantly vary in S cells deprived from either FGF, EGF, B27 or heparin for 3 days (Fig. 4E), a time-point where the switch to DMEM had already strongly decreased MGMT levels (Fig. 4A). Moreover, FCS deprivation did not induce MGMT in GS-5 maintained in monolayer conditions; neither did the addition of FCS alone to NB medium significantly decrease MGMT levels (Fig. 4E). Although the media supplements, either in NB medium as growth factors or in DMEM as FCS appeared to have no direct impact on MGMT expression *per se*, cell morphology was quite dependent on the medium in which the cells were grown (Fig. 4F), and cells neither attached in DMEM without FCS nor formed spheres in NB without supplements. To finally exclude that attachment or detachment regulate MGMT expression levels, we cultured GIC sphere cells in complete NB medium for up to 6 days either with or without supplementation of 10% FCS to induce attachment. However, only a minor reduction of MGMT protein levels was observed upon attachment (Fig. 4G,H).

To exclude a sole effect of induction of attachment by FCS in this context, expression of MGMT under modulation of attachment by the integrin inhibitors cilengitide or GLPG0187 was analysed. No significant regulation of MGMT, neither on mRNA nor protein level, was observed in S or M cells exposed to either integrin inhibitor (Supplementary Fig. 2A,B). Single-cell gene expression analysis did not confirm negative correlations for expression of MGMT versus that of several adhesion molecules (Supplementary Fig. 2C). Additionally, to exclude that GIC cells under S conditions express higher levels of MGMT due to higher hypoxia levels within the spheres, driving the cells into a more stem cell state, we analysed MGMT expression levels in MGMT-expressing LTC or GIC. Intriguingly, cells kept under hypoxic conditions displayed reduced levels of MGMT on both mRNA and protein levels. Induction of hypoxia was verified by expression analysis of the hypoxia marker, carbonic anhydrase 9 (CAIX), which also confirmed higher baseline levels of hypoxia in S cultures (Supplementary Fig. 2D-F). Finally, sphere formation capacity was not impacted by silencing of MGMT or by O^6-BG-mediated MGMT consumption (Supplementary Fig. 3A-C).

NF-κB, a transcriptional regulator of MGMT, is overexpressed in GIC

NF-κB is a transcription factor previously described to be a positive regulator of MGMT (Lavon *et al.*, 2007). Therefore, we investigated whether NF-κB impacts MGMT regulation in human GIC cells as well. Expression of NF-κB did not differ consistently in GS-2 and GS-5 S versus M cells on mRNA levels; however, NF-κB subunit p65 protein levels were increased in S cells of GS-2 and GS-5 (Fig. 5A). Moreover, we confirmed a higher activity of NF-κB in S cells by luciferase reporter assay in GS-2 and GS-5 S versus M cells, an activity that was suppressed by pre-exposure to the NF-κB inhibitor, BAY 11-7082 (Fig. 5B). Likewise, pre-exposure to

BAY 11-7082 significantly reduced MGMT protein levels in a concentration-dependent manner for at least 72 h in GS-2, GS-5, T-325 and ZH-161 (Fig. 5C); in the latter cell lines, higher concentrations of the inhibitor did, however, result in cell death (data not shown), as reflected by protein degradation shown as a gradual loss of actin (Fig. 5C). Likewise, GIC exposure to moderate concentrations of BAY 11-7082 over a longer period in the context of spherogenicity assays resulted in evolution of cell death after seven days, demonstrating the prosurvival function of NF-κB, but precluding formal analyses of BAY 11-7082-mediated sensitization to TMZ in spherogenicity assays (data not shown). We confirmed the NF-κB-mediated regulation of MGMT by an siRNA-mediated approach using p50/p65si to silence NF-κB expression (Fig. 5D). A second siRNA pool was used to validate the results in GS-2, GS-5, T-325 and ZH-161 cells (Fig. 5E).

MGMT expression pattern in LTC

To better understand this hitherto undescribed regulation of MGMT expression, we next asked whether the differential expression of MGMT in S versus M cultures was specific to the GIC phenotype. LN-18 and T98G cells, the only MGMT-expressing LTC in our panel (Hermisson et al. 2006), formed spheres when grown in NB medium, and displayed a strong increase in MGMT levels when shifted to S conditions (Supplementary Fig. 4A,B). Similar experiments were performed as a control for two further LTC, LN-229 and LN-308, which do not express MGMT as a result of MGMT promoter methylation (Supplementary Fig. 4C). S cultures of these cells did not acquire MGMT expression (Supplementary Fig. 4D). Again, silencing of MGMT in MGMT-expressing LN-18 cells, or overexpression of MGMT in methylated LN-229 cells, did not impact their sphere formation capacity (Supplementary Fig. 4E,F). LN-229 cells engineered to overexpress MGMT showed a higher level of TMZ

resistance than control cells under either conditions, although the M-to-S shift per se conferred increased TMZ resistance in the absence of MGMT induction (Supplementary Fig. 4G).

Discussion

The role of *MGMT* promoter methylation as a predictor of benefit from alkylating chemotherapy in glioblastoma is well established (Weller *et al.* 2010). Further, the impact of GIC for maintenance of the malignant phenotype of gliomas has been studied extensively over the last years (Lathia et al. 2015). Yet, the regulation of MGMT expression in GIC has remained poorly understood.

Here, we report that GIC cultures transferred from S to M culture conditions exhibit reduced MGMT expression (Fig. 2A,B) associated with enhanced sensitivity to TMZ (Fig. 2C-E). Increased TMZ resistance in S cells was not merely linked to reduced exposure of sphere cells to TMZ, compared with M cells which grow as a flat monolayer, since there was no increase in the resistance to TMZ from M to S cells in the two cell lines lacking MGMT expression, GS-9 and ZH-305. The changes in MGMT expression in cells lacking *MGMT* promoter methylation could be linked neither to direct stimulating effect of a specific component of the sphere culture medium nor to a suppressive effect of FCS (Fig. 4). A relevant association of MGMT expression with cell attachment or higher MGMT expression caused by hypoxia within the spheres was excluded, too (Supplementary Fig. 2). Interestingly, the same pattern of increased MGMT protein expression was seen in 2 LTC lacking *MGMT* promoter methylation when grown in sphere conditions (Supplementary Fig. 4A,B). However, MGMT expression and sphere formation appear not to be directly linked, as depletion of MGMT by either gene silencing or consumption by the pharmacological inhibitor O^6-BG did not result in impaired sphere formation of the cells, neither in GIC nor LTC (Supplementary Fig. 3, Supplementary Fig. 4E). In glioblastoma cells isolated from freshly resected tumor tissue and sorted for the stem cell marker CD133, increased MGMT expression was found in the CD133-positive

population (Fig. 3B) (Liu *et al.* 2006). Admittedly, CD133 remains a controversial stem cell marker (Beier *et al.* 2007); however, lacking a more reliable validated marker, sorting for CD133 remained a practicable approach for fresh tumor tissue. Moreover, a positive correlation between MGMT and common stemness markers was confirmed by single cell gene PCR, too (Fig. 3A).

NF-κB, a transcription factor regulating cell survival and proliferation in several tumor entities (Naugler & Karin 2008), is also constitutively active in malignant brain tumors. It has been linked to epidermal growth factor receptor activity in glioblastoma via the PI3-kinase/Akt signalling axis (Kapoor *et al.* 2004), as well as to resistance to tumor necrosis factor-related apoptosis-inducing ligand-mediated apoptotic cell death (Bredel *et al.* 2006). Pharmacological inhibition of NF-kB was shown to induce cell death preferentially in glioblastoma cells and not in normal astrocytes (Zanotto-Filho *et al.* 2011). Overall, NF-kB has emerged as a focus of research for therapeutic approaches to block its downstream signalling pathway, and thus represents a potential target in tumor therapy. Several direct or indirect NF-kB inhibitors are available, such as sulfasalazine (Hermisson & Weller 2003), some of which have been used in clinical trials in chronic inflammatory disorders with clinical benefit and tolerable side effects (Combe *et al.* 2009). Positive effects were additionally seen for long-term outcome in patients with rheumatoid diseases, with sustained benefits of persistent disease suppression in follow-up studies after several years (van Rossum *et al.* 2007). A phase 1/2 prospective study using sulfasalazine in progressive WHO III or IV glioma was terminated early after the interim analysis; however, as the investigated cohort comprised 10 patients until termination, all with recurrent, large tumors and low Karnofsky performance score (median KPS: 50), those results must be interpreted with caution (Robe *et al.* 2009). Finally, NF-kB has been described as a regulator of MGMT expression in glioma cells (Lavon *et al.* 2007). In our model, we

confirmed a decrease in MGMT protein levels after inhibition of NF-kB, either by pharmacological inhibition or by a siRNA-mediated approach, therefore linking NF-kB to MGMT expression in GIC cells cultured under S conditions (Fig. 5). The NF-κB inhibitor BAY 11-7082 however induced global cell death of inhibitor-exposed cells over several days (Fig. 5C) and prohibited comparative viability assays, probably due to the utmost importance of this transcription factor for cell survival, preventing any cell growth after its complete blockage. Still, NF-kB emerges as a responsible regulator of MGMT expression in GIC S cells in our model, making this transcription factor an even more relevant putative target to therapeutic approaches, considering the indisputable relevance of stem-like cells for glioblastoma malignancy and their high resistance to therapy.

Funding statement

Supported by a grant from the Wilhelm Sander Foundation for Cancer Research to MW and GR (2012.088.1).

Acknowledgement

The authors thank K. Lamszus (Hamburg, Germany) for providing the GS cell lines, and I. Burghardt and E. Ventura (Zurich, Switzerland) for sharing single cell expression data for this study.

Conflict of interest

The authors declare no conflict of interest related to this manuscript. MW is a handling editor for the journal.

References

Beier, D., Hau, P., Proescholdt, M. et al. (2007) CD133(+) and CD133(-) glioblastoma-derived cancer stem cells show differential growth characteristics and molecular profiles. *Cancer research,* **67,** 4010-4015.

Beier, D., Rohrl, S., Pillai, D. R. et al. (2008) Temozolomide preferentially depletes cancer stem cells in glioblastoma. *Cancer research,* **68,** 5706-5715.

Bleau, A. M., Hambardzumyan, D., Ozawa, T., Fomchenko, E. I., Huse, J. T., Brennan, C. W. and Holland, E. C. (2009) PTEN/PI3K/Akt pathway regulates the side population phenotype and ABCG2 activity in glioma tumor stem-like cells. *Cell Stem Cell,* **4,** 226-235.

Blough, M. D., Westgate, M. R., Beauchamp, D., Kelly, J. J., Stechishin, O., Ramirez, A. L., Weiss, S. and Cairncross, J. G. (2010) Sensitivity to temozolomide in brain tumor initiating cells. *Neuro-Oncology,* **12,** 756-760.

Bredel, M., Bredel, C., Juric, D. et al. (2006) Tumor necrosis factor-alpha-induced protein 3 as a putative regulator of nuclear factor-kappaB-mediated resistance to O6-alkylating agents in human glioblastomas. *J Clin Oncol,* **24,** 274-287.

Combe, B., Codreanu, C., Fiocco, U. et al. (2009) Efficacy, safety and patient-reported outcomes of combination etanercept and sulfasalazine versus etanercept alone in patients with rheumatoid arthritis: a double-blind randomised 2-year study. *Ann Rheum Dis,* **68,** 1146-1152.

Golebiewska, A., Bougnaud, S., Stieber, D. et al. (2013) Side population in human glioblastoma is non-tumorigenic and characterizes brain endothelial cells. *Brain,* **136,** 1462-1475.

Gramatzki, D., Dehler, S., Rushing, E. J. et al. (2016) Glioblastoma in the Canton of Zurich, Switzerland revisited: 2005 to 2009. *Cancer,* **122,** 2206-2215.

Gunther, H. S., Schmidt, N. O., Phillips, H. S. et al. (2008) Glioblastoma-derived stem cell-enriched cultures form distinct subgroups according to molecular and phenotypic criteria. *Oncogene,* **27,** 2897-2909.

Happold, C., Roth, P., Wick, W., Schmidt, N., Florea, A. M., Silginer, M., Reifenberger, G. and Weller, M. (2012) Distinct molecular mechanisms of acquired resistance to temozolomide in glioblastoma cells. *Journal of neurochemistry,* **122,** 444-455.

Hegi, M. E., Diserens, A. C., Gorlia, T. et al. (2005) MGMT gene silencing and benefit from temozolomide in glioblastoma. *The New England journal of medicine,* **352,** 997-1003.

Hermisson, M., Klumpp, A., Wick, W., Wischhusen, J., Nagel, G., Roos, W., Kaina, B. and Weller, M. (2006) O6-methylguanine DNA methyltransferase and p53 status predict temozolomide sensitivity in human malignant glioma cells. *Journal of neurochemistry,* **96,** 766-776.

Hermisson, M. and Weller, M. (2003) NF-kappaB-independent actions of sulfasalazine dissociate the CD95L- and Apo2L/TRAIL-dependent death signaling pathways in human malignant glioma cells. *Cell Death Differ,* **10,** 1078-1089.

Johnson, D. R. and O'Neill, B. P. (2012) Glioblastoma survival in the United States before and during the temozolomide era. *Journal of neuro-oncology,* **107,** 359-364.

Kapoor, G. S., Zhan, Y., Johnson, G. R. and O'Rourke, D. M. (2004) Distinct domains in the SHP-2 phosphatase differentially regulate epidermal growth factor receptor/NF-kappaB activation through Gab1 in glioblastoma cells. *Mol Cell Biol,* **24,** 823-836.

Lathia, J. D., Mack, S. C., Mulkearns-Hubert, E. E., Valentim, C. L. and Rich, J. N. (2015) Cancer stem cells in glioblastoma. *Genes Dev,* **29,** 1203-1217.

Lavon, I., Fuchs, D., Zrihan, D., Efroni, G., Zelikovitch, B., Fellig, Y. and Siegal, T. (2007) Novel mechanism whereby nuclear factor kappaB mediates DNA damage repair through regulation of O(6)-methylguanine-DNA-methyltransferase. *Cancer research,* **67,** 8952-8959.

Lemke, D., Weiler, M., Blaes, J. et al. (2014) Primary glioblastoma cultures: can profiling of stem cell markers predict radiotherapy sensitivity? *Journal of neurochemistry,* **131,** 251-264.

Liu, G., Yuan, X., Zeng, Z. et al. (2006) Analysis of gene expression and chemoresistance of CD133+ cancer stem cells in glioblastoma. *Mol Cancer,* **5,** 67.

Naugler, W. E. and Karin, M. (2008) NF-kappaB and cancer-identifying targets and mechanisms. *Curr Opin Genet Dev,* **18,** 19-26.

Papa, E., Weller, M., Weiss, T., Ventura, E., Burghardt, I. and Szabo, E. (2017) Negative control of the HGF/c-MET pathway by TGF-beta: a new look at the regulation of stemness in glioblastoma. *Cell Death Dis,* **8,** 3210.

Robe, P. A., Martin, D. H., Nguyen-Khac, M. T. et al. (2009) Early termination of ISRCTN45828668, a phase 1/2 prospective, randomized study of sulfasalazine for the treatment of progressing malignant gliomas in adults. *BMC Cancer,* **9,** 372.

Sciuscio, D., Diserens, A. C., van Dommelen, K. et al. (2011) Extent and patterns of MGMT promoter methylation in glioblastoma- and respective glioblastoma-derived spheres. *Clinical cancer research : an official journal of the American Association for Cancer Research,* **17,** 255-266.

Silginer, M., Burghardt, I., Gramatzki, D. et al. (2016) The aryl hydrocarbon receptor links integrin signaling to the TGF-beta pathway. *Oncogene,* **35,** 3260-3271.

Stahlberg, A., Rusnakova, V., Forootan, A., Anderova, M. and Kubista, M. (2013) RT-qPCR work-flow for single-cell data analysis. *Methods,* **59,** 80-88.

Stojcheva, N., Schechtmann, G., Sass, S. et al. (2016) MicroRNA-138 promotes acquired alkylator resistance in glioblastoma by targeting the Bcl-2-interacting mediator BIM. *Oncotarget,* **7,** 12937-12950.

van Rossum, M. A., van Soesbergen, R. M., Boers, M. et al. (2007) Long-term outcome of juvenile idiopathic arthritis following a placebo-controlled trial: sustained benefits of early sulfasalazine treatment. *Ann Rheum Dis,* **66,** 1518-1524.

Weller, M., Stupp, R., Reifenberger, G., Brandes, A. A., van den Bent, M. J., Wick, W. and Hegi, M. E. (2010) MGMT promoter methylation in malignant gliomas: ready for personalized medicine? *Nat Rev Neurol,* **6,** 39-51.

Weller, M., van den Bent, M., Tonn, J. C. et al. (2017) European Association for Neuro-Oncology (EANO) guideline on the diagnosis and treatment of adult astrocytic and oligodendroglial gliomas. *The lancet oncology,* **18,** e315-e329.

Zanotto-Filho, A., Braganhol, E., Schroder, R., de Souza, L. H., Dalmolin, R. J., Pasquali, M. A., Gelain, D. P., Battastini, A. M. and Moreira, J. C. (2011) NFkappaB inhibitors induce cell death in glioblastomas. *Biochem Pharmacol,* **81,** 412-424.

Figure legends

Fig. 1. TMZ resistance of sphere cultures. A. GS-2 or GS-5 maintained as S (NB medium) or M (DMEM) (phase-contrast microscopy; size bar: 200 µm). B. mRNA expression levels of GFAP and CD133 in GS-2 or GS-5 GIC S or M were assessed by qPCR. C,D. GS-2 or GS-5 GIC grown as S or M cultures were exposed to increasing concentrations of TMZ for 24 h and allowed to grow for 2 weeks after removal of TMZ (S, white squares; M, black diamonds). Clonogenic survival was assessed by MTT assay for S and by crystal violet assay for M cultures. Data are expressed as mean ± SEM (n=3) ($p<0.05$, *; $p<0.01$, **; $p<0.001$, ***). E. EC_{50} values for GIC were determined for TMZ under S (white bars) or M (black bars) conditions (log scale) (n=3). F. Cell cycle analyses were performed by flow cytometry in GS-2 and GS-5 S or M cells; cell cycle distributions are displayed as bar graphs (black, sub-G1; dark grey, G1; light grey, S; white, G2/M) (n=3). G. GS-2 and GS-5 S or M cells were seeded with 6 well replicates per time point and assessed for proliferation rates at 24 h (dark grey), 48 h (light grey) and 72 h (grey). Values were normalized to baseline for each cell lines.

Fig. 2. MGMT-mediated TMZ resistance in GIC cultures. A. *MGMT* mRNA expression was assessed by qPCR (S, white bars; M, black bars) (n=3). B. MGMT protein levels were determined by immunoblot of lysates of S versus M cultures. β-Actin was used as loading control. MGMT-negative LN-229 and MGMT-positive LN-18 as well as highly MGMT-positive LN-18_R cells (Happold et al. 2012) were used as negative and positive controls (n=2). C. Correlation between the EC_{50} values and MGMT mRNA levels was plotted and calculated by Spearman test for S and M cells. D. GS-2 or GS-5 cells were seeded under S or M conditions, treated with 50 µM O^6-

BG or DMSO control for 2 h, exposed to TMZ after removal of O^6-BG for 24 h at increasing concentrations, and allowed to grow for 2 weeks (S without O^6-BG: white squares; S with O^6-BG: grey squares; M without O^6-BG: black diamonds; M with O^6-BG: grey diamonds) (n=3). MGMT protein levels GS-2 S cells exposed to O^6-BG (50 µM) or DMSO control were assessed by immunoblot after 72 h.

Fig. 3. Pattern of stemness and differentiation in MGMT-expressing GIC. A. Correlations among MGMT and stem cell markers in single cell qRT-PCR analysis were determined in freshly resected glioblastoma tissues. Significant positive Pearson correlations are represented by blue ellipses. Crosses indicate non-significant correlations. B. MGMT mRNA expression was assessed by qPCR in cells isolated from freshly resected tumor tissue from patients with glioblastoma; cells were sorted for presence (white bars) versus absence (black bars) of CD133 expression (n=1). C. GS-2, GS-5, T-325 or ZH-161 S cells were exposed to BMP-4 at 100 ng/ml for 72 h. MGMT protein levels were assessed by immunoblot. D. CD133 or GFAP mRNA expression were assessed by qPCR in GS-2, GS-5, T-325 or ZH-161 (without BMP-4, white bars; with BMP-4, black bars (n=2).

Fig. 4. Regulation of *MGMT* expression by cell culture conditions. A. GS-2 or GS-5 S cells were transferred to DMEM and assessed for MGMT levels by immunoblot at the indicated time points. Respective GS S cells kept in NB medium served as control. B. GS-2 or GS-5 M were transferred to NB medium and assessed for MGMT levels by immunoblot. Respective GS M in DMEM served as control. C. GS-2 S cells were grown in either NB fully supplemented (NB-full) or pure NB medium (NB-empty) for 24, 48, 72 or 96 h, and MGMT protein levels were assessed by immunoblot. D. Viability was assessed at corresponding time points to Fig. 4C by

trypan blue exclusion assay. E. GS-5 S cells cultured in NB were transferred to NB medium deprived of (w/o) either supplement for 72 h and assessed for MGMT protein levels by immunoblot. GS-5 M cells in DMEM and GS-5 S cells in NB supplemented with 5% FCS served as a controls. F. Phase-contrast microscopy of GS-2 cells cultured in different conditions (scale 100 µm). G. GS-5 S cells were cultured in NB or NB with 5% FCS for 48 h, 96 h or 144 h, respectively. MGMT protein levels were assessed by immunoblot. H. Corresponding culture imaging (magnification 200 µm).

Fig. 5. Transcriptional regulation of MGMT: a role for NF-kB. A. mRNA expression levels of NF-kB subunit p65 were assessed by qPCR for GS-2 and GS-5 S and M cells. White bars, S cultures; black bars, M cultures (left panel). NF-kB subunit p65 protein levels were assessed by immunoblot in these cells (right panel). B. Luciferase reporter assays were performed in GS-2 and GS-5 S or M cells exposed to either BAY 11-7082 (15 µM) or control. Normalized luciferase expression indicates NF-kB activity. Plates were stopped 24 h after plasmid transfection and 6 h after inhibitor exposure. C. GS-2, GS-5, T-325 or ZH-161 S cells exposed to the NF-kB inhibitor BAY 11-7082 at increasing concentrations as indicated or DMSO control were assessed for MGMT protein levels by immunoblot at different time points. Actin served as control. D. GS-2 or GS-5 cells were transfected either with NF-kB subunits p50/p65 siRNA or scrambled control and MGMT protein levels were assessed at different time points; gene silencing of p50/p65 was confirmed on protein levels. Actin served as control. E. The same cells as in C were transfected either with another siRNA pool for NF-kB subunits p50/p65 or scrambled control and MGMT protein levels were assessed. Actin served as control.

Fig 1

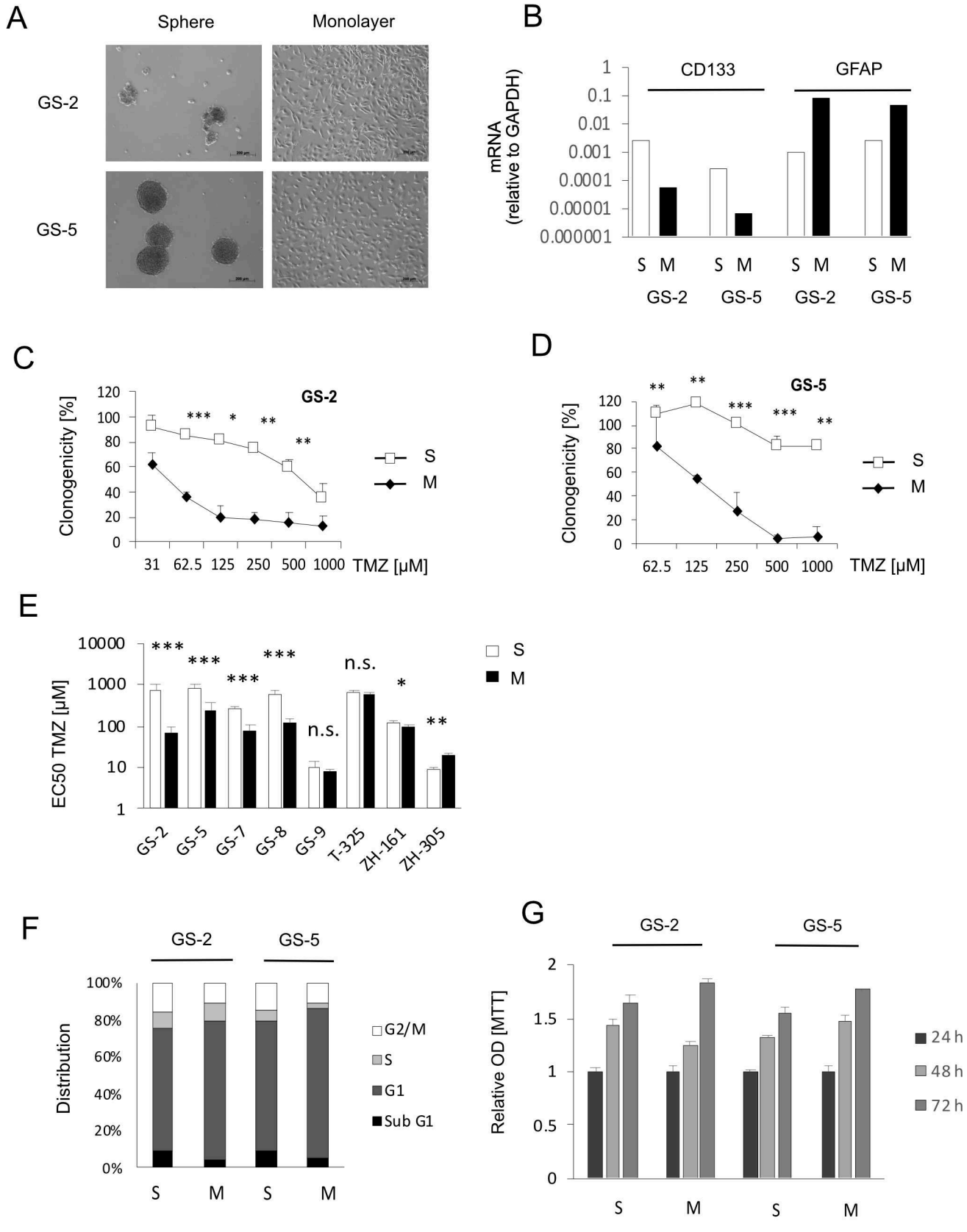
A
Sphere
Monolayer
GS-2
GS-5
B
CD133
GFAP
mRNA (relative to GAPDH)
1
0.1
0.01
0.001
0.0001
0.00001
0.000001
S M S M S M S M
GS-2 GS-5 GS-2 GS-5
C
GS-2
Clonogenicity [%]
120
100
80
60
40
20
0
***
*
**
**
S
M
31 62.5 125 250 500 1000 TMZ [μM]
D
GS-5
**
**
***
***
**
Clonogenicity [%]
120
100
80
60
40
20
0
S
M
62.5 125 250 500 1000 TMZ [μM]
E
EC50 TMZ [μM]
10000
1000
100
10
1
***
***
***
***
n.s.
n.s.
*
**
S
M
GS-2 GS-5 GS-7 GS-8 GS-9 T-325 ZH-161 ZH-305
F
GS-2
GS-5
Distribution
100%
80%
60%
40%
20%
0%
G2/M
S
G1
Sub G1
S M S M
G
GS-2
GS-5
Relative OD [MTT]
2
1.5
1
0.5
0
24 h
48 h
72 h
S M S M

Fig 5

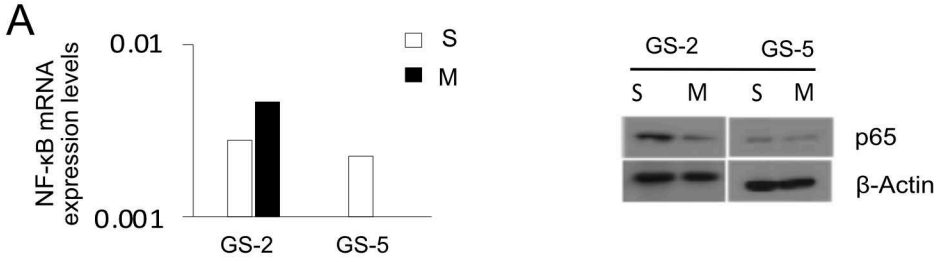
A
NF-κB mRNA expression levels
0.01
0.001
S
M
GS-2
GS-5
GS-2
GS-5
S
M
S
M
p65
β-Actin

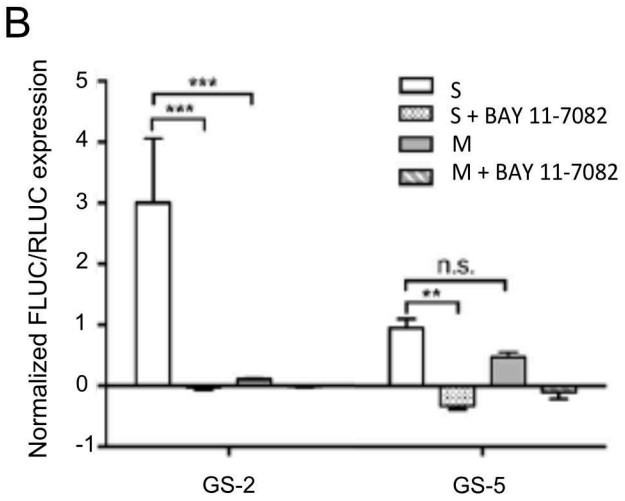
B
Normalized FLUC/RLUC expression
5
4
3
2
1
0
-1
***
***
n.s.
**
S
S + BAY 11-7082
M
M + BAY 11-7082
GS-2
GS-5

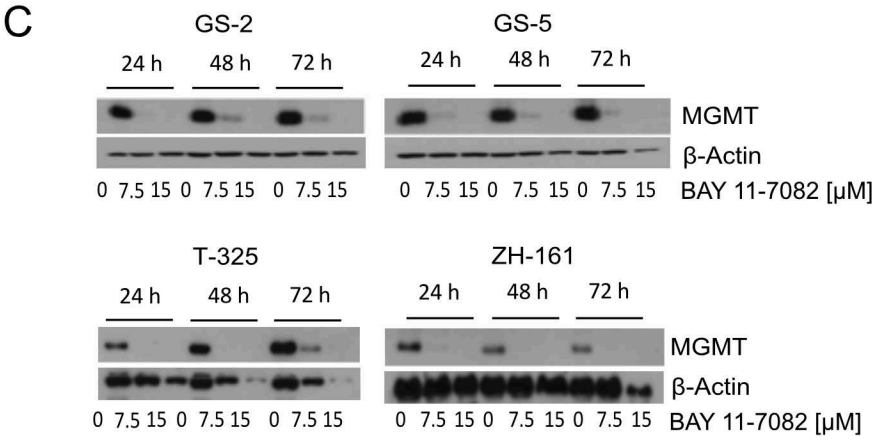
C
GS-2
GS-5
24 h
48 h
72 h
MGMT
β-Actin
0 7.5 15 0 7.5 15 0 7.5 15
BAY 11-7082 [μM]
T-325
ZH-161

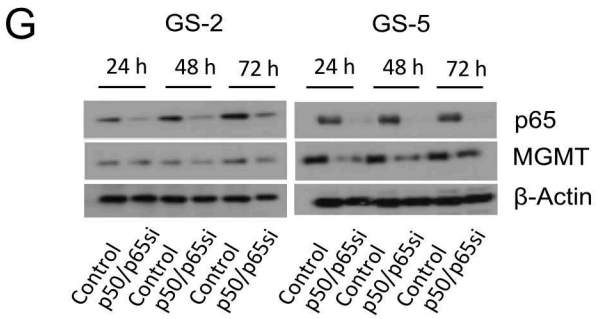
G
GS-2
GS-5
24 h
48 h
72 h
p65
MGMT
β-Actin
Control
p50/p65si

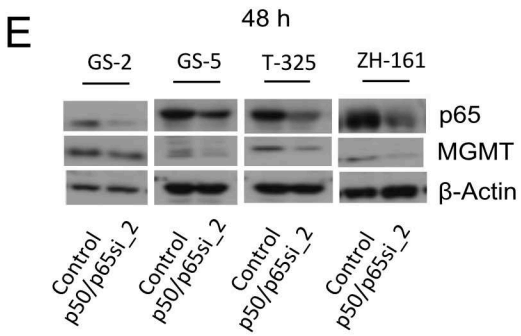
E
48 h
GS-2
GS-5
T-325
ZH-161
p65
MGMT
β-Actin
Control
p50/p65si_2

Fig 4

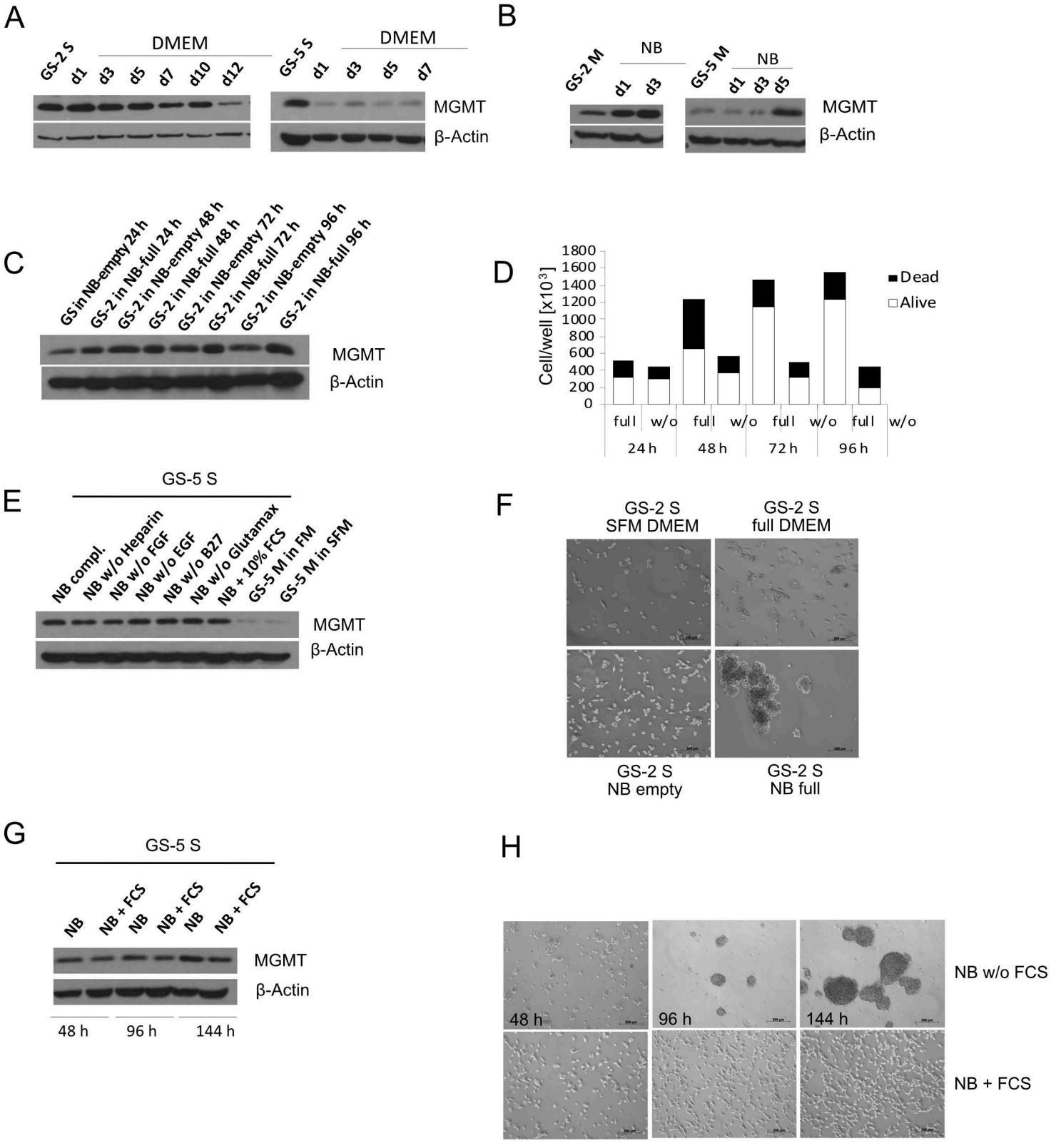
A
GS-2 S
DMEM
d1
d3
d5
d7
d10
d12
GS-5 S
DMEM
d1
d3
d5
d7
MGMT
β-Actin
B
GS-2 M
NB
d1
d3
GS-5 M
NB
d1
d3
d5
MGMT
β-Actin
C
GS in NB-empty 24 h
GS-2 in NB-full 24 h
GS-2 in NB-empty 48 h
GS-2 in NB-full 48 h
GS-2 in NB-empty 72 h
GS-2 in NB-full 72 h
GS-2 in NB-empty 96 h
GS-2 in NB-full 96 h
MGMT
β-Actin
D
Cell/well [x10³]
1800
1600
1400
1200
1000
800
600
400
200
0
Dead
Alive
full
w/o
full
w/o
full
w/o
full
w/o
24 h
48 h
72 h
96 h
E
GS-5 S
NB compl.
NB w/o Heparin
NB w/o FGF
NB w/o EGF
NB w/o B27
NB w/o Glutamax
NB + 10% FCS
GS-5 M in FM
GS-5 M in SFM
MGMT
β-Actin
F
GS-2 S
SFM DMEM
GS-2 S
full DMEM
GS-2 S
NB empty
GS-2 S
NB full
G
GS-5 S
NB
NB + FCS
NB
NB + FCS
NB
NB + FCS
MGMT
β-Actin
48 h
96 h
144 h
H
48 h
96 h
144 h
NB w/o FCS
NB + FCS

Fig 3

A

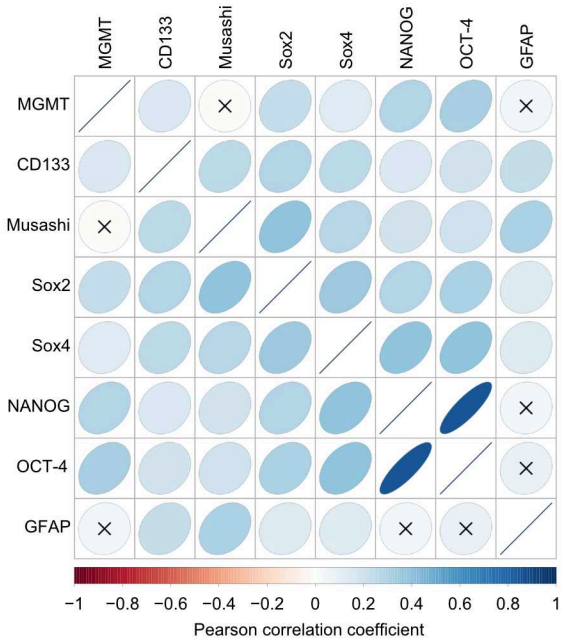
MGMT
CD133
Musashi
Sox2
Sox4
NANOG
OCT-4
GFAP
−1 −0.8 −0.6 −0.4 −0.2 0 0.2 0.4 0.6 0.8 1
Pearson correlation coefficient

B

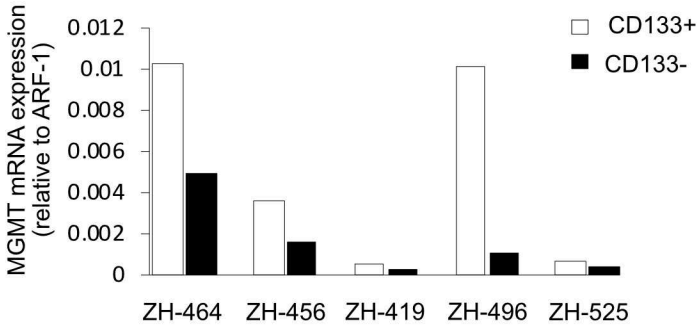
MGMT mRNA expression (relative to ARF-1)
0.012
0.01
0.008
0.006
0.004
0.002
0
CD133+
CD133-
ZH-464 ZH-456 ZH-419 ZH-496 ZH-525

C

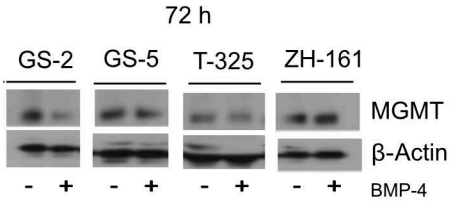
72 h
GS-2 GS-5 T-325 ZH-161
MGMT
β-Actin
- + - + - + - +
BMP-4

D

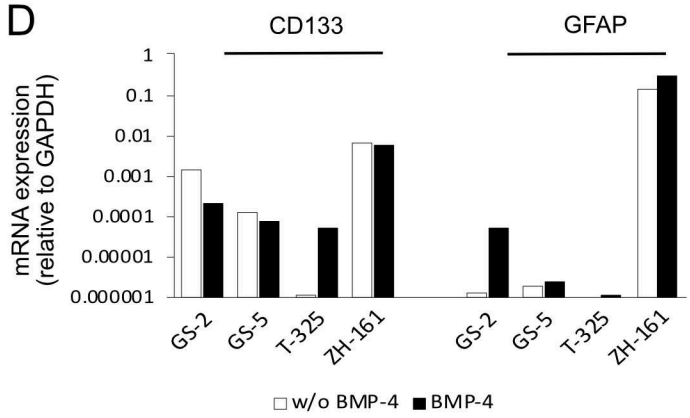
CD133
GFAP
mRNA expression (relative to GAPDH)
1
0.1
0.01
0.001
0.0001
0.00001
0.000001
GS-2 GS-5 T-325 ZH-161 GS-2 GS-5 T-325 ZH-161
w/o BMP-4
BMP-4

Fig 2

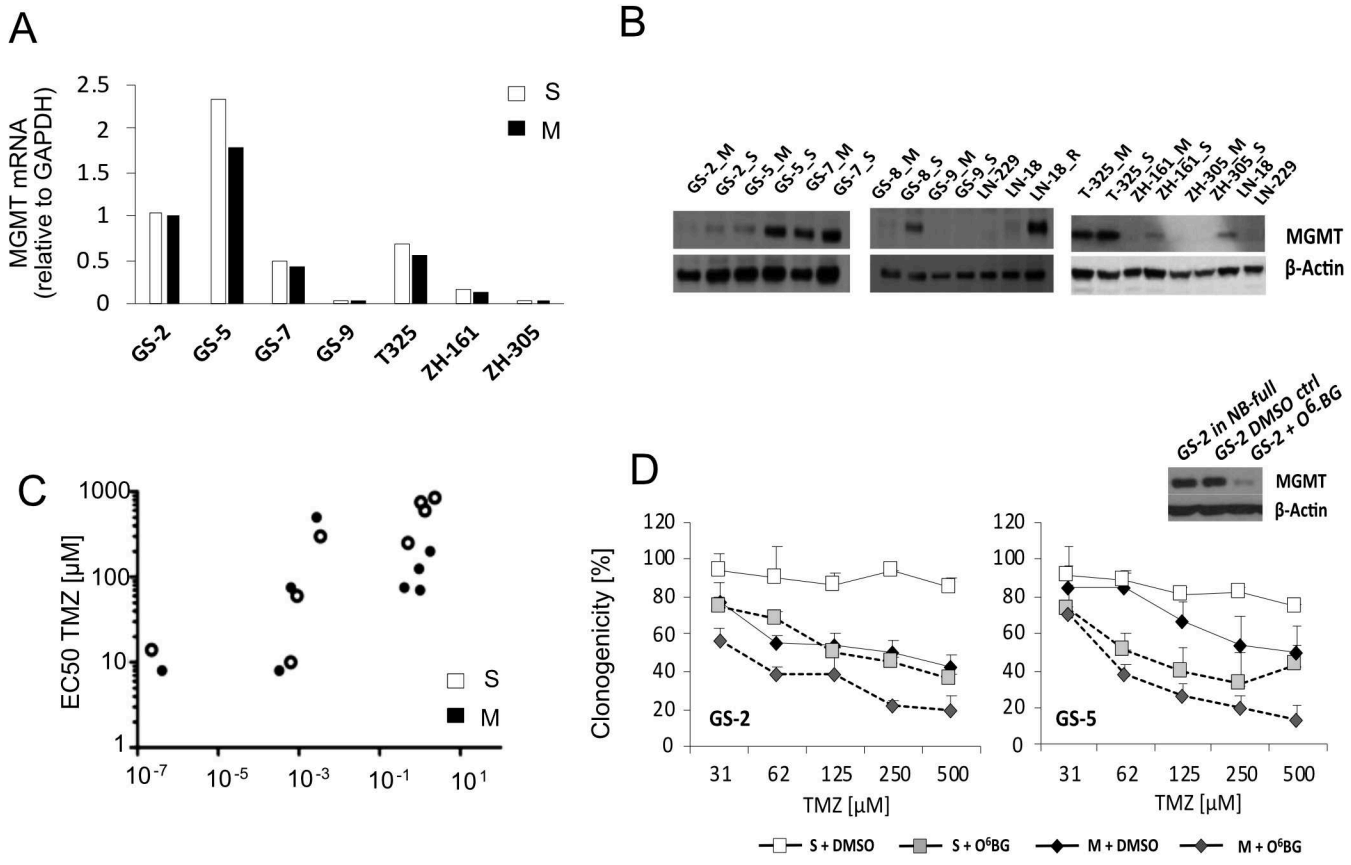
A
MGMT mRNA (relative to GAPDH)
2.5
2
1.5
1
0.5
0
S
M
GS-2
GS-5
GS-7
GS-9
T325
ZH-161
ZH-305
B
GS-2_M
GS-2_S
GS-5_M
GS-5_S
GS-7_M
GS-7_S
GS-8_M
GS-8_S
GS-9_M
GS-9_S
LN-229
LN-18
LN-18_R
T-325_M
T-325_S
ZH-161_M
ZH-161_S
ZH-305_M
ZH-305_S
LN-18
LN-229
MGMT
β-Actin
C
EC50 TMZ [µM]
1000
100
10
1
10^{-7}
10^{-5}
10^{-3}
10^{-1}
10^{1}
S
M
D
GS-2 in NB-full
GS-2 DMSO ctrl
GS-2 + O6-BG
MGMT
β-Actin
Clonogenicity [%]
120
100
80
60
40
20
0
GS-2
GS-5
31
62
125
250
500
TMZ [µM]
S + DMSO
S + O6BG
M + DMSO
M + O6BG

Transcriptional control of O^6-methylguanine DNA methyltransferase expression and temozolomide resistance in glioblastoma

Caroline Happold[1], Nina Stojcheva[1], Manuela Silginer[1], Tobias Weiss[1], Patrick Roth[1], Guido Reifenberger[2], Michael Weller[1]

[1]Laboratory of Molecular Neuro-Oncology, Department of Neurology, University Hospital and University of Zurich, Zurich, Frauenklinikstrasse 26, and Neuroscience Center Zurich, University of Zurich, 8091 Zurich, Switzerland; [2]Department of Neuropathology, Heinrich-Heine-University Düsseldorf, Düsseldorf, and German Cancer Consortium (DKTK), partner site Essen/Düsseldorf, Germany

Supplementary Figures

Supplementary Fig. 1. Stem cell and differentiation marker expression, cell death and viability in M and S cells

Supplementary Fig. 2. MGMT regulation: effects of cell adhesion and hypoxia

Supplementary Fig. 3. Sphere-formation capacity does not depend on MGMT expression

Supplementary Fig. 4. MGMT regulation in sphere-forming LTC

Supplementary Fig. 1

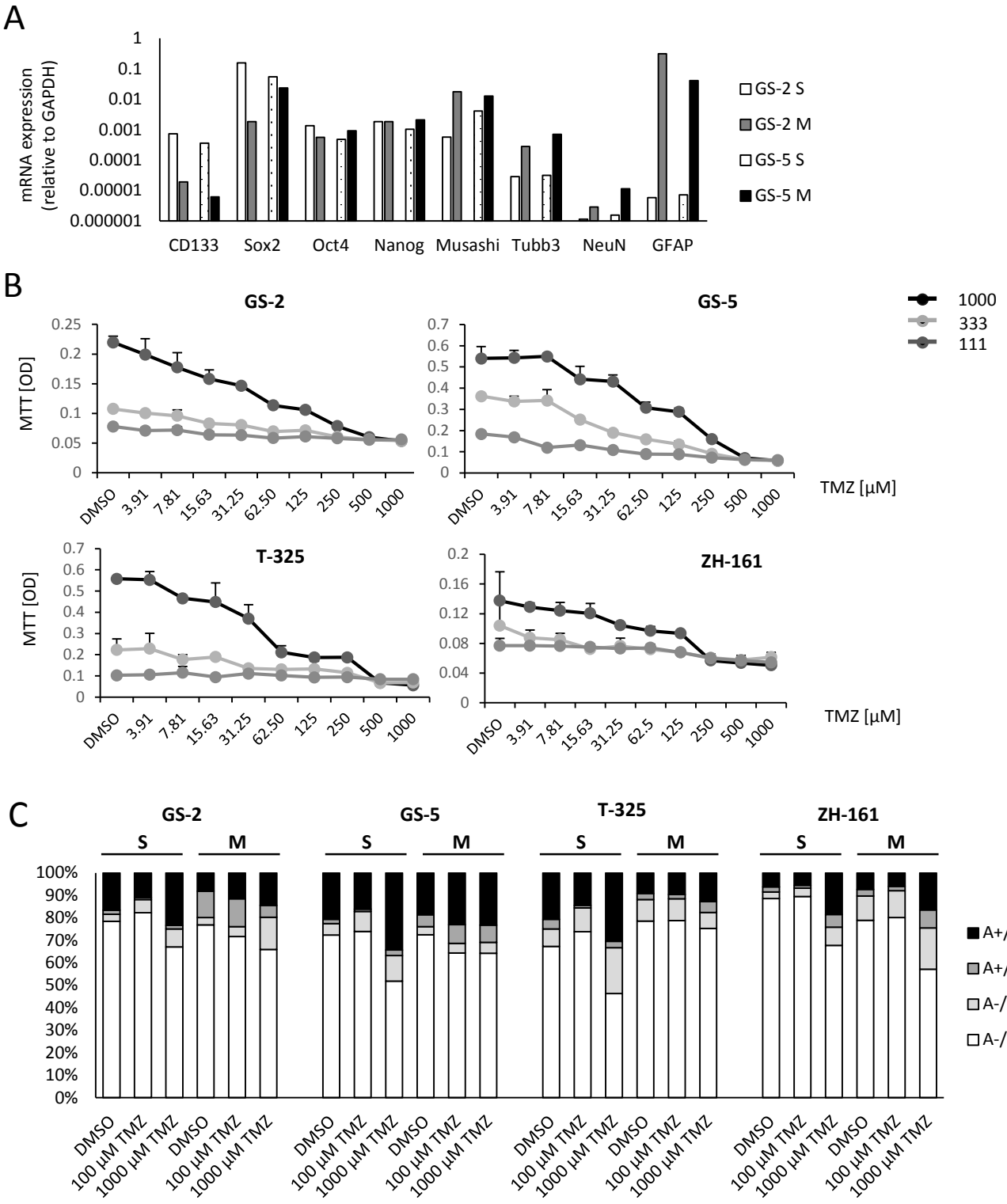

Supplementary Fig. 1. Stem cell and differentiation marker expression, cell death and viability in S and M cells. A. mRNA expression levels of CD133, Sox2, Oct4, Nanog, Musashi, Tubb3, NeuN and GFAP in GS-2 or GS-5 GIC S or M were assessed by qPCR (GS-2 S, white; GS-5 S, white dotted; GS-2 M, dark grey; GS-5 M, black). B. Limiting dilution assays were performed in GS-2, GS-5, T-325 or ZH-161 cells seeded at either 1000, 333 or 111 cells per well, and exposed to TMZ in the indicated concentrations. C. GS-2, GS-5, T-325 or ZH-161 cells were exposed to either DMSO control or TMZ at 100 or 1000 µM for 24 h and allowed to grow for 10-14 days. Cell death was assessed by Annexin V/PI staining (Anx/PI -/-, white; Anx/PI +/-, dark grey; Anx/PI -/+, light grey; Anx/PI +/+, black).

Supplementary Fig 2

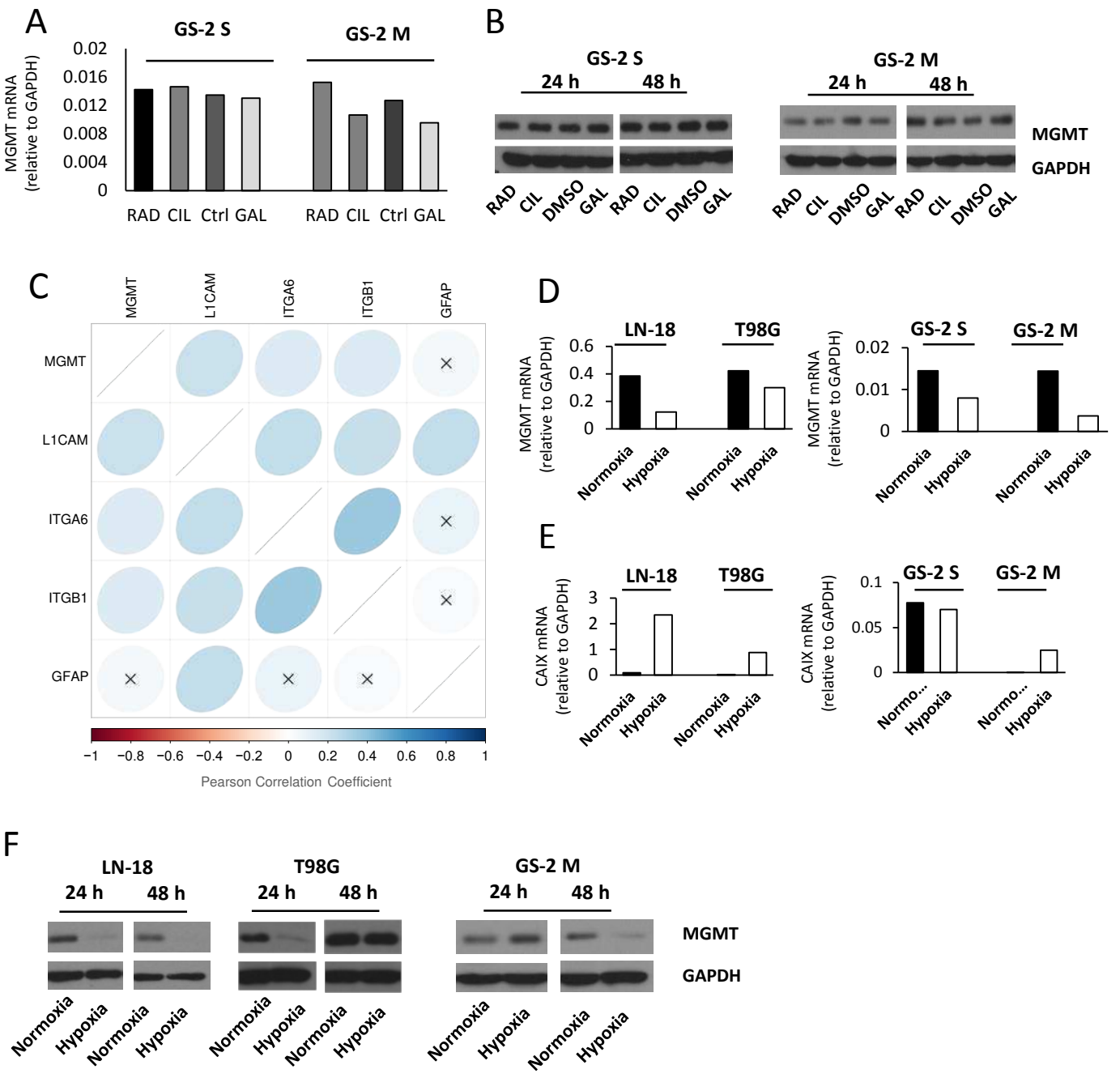

Supplementary Fig. 2. MGMT regulation: effects of cell adhesion and hypoxia. A, B. GS-2 cells kept under S or M conditions were exposed to RAD (10 µM), cilengitide (10 µM) or GLPG0187 (1 nM). *MGMT* mRNA expression was assessed by qPCR at 24 h (A); MGMT protein levels were assessed at 24 h or 48 h by immunoblot (B). C. Correlation analysis was performed for MGMT and cell adhesion markers in single cell qRT-PCR analysis using freshly resected glioblastoma tissues. Positive Pearson correlations are represented by blue ellipses. Crosses indicate non-significant correlations. D. MGMT-expressing LTC (LN-18 or T98G) and GIC cells kept either under S or M conditions were maintained under hypoxic or normoxic conditions for 24 h, and MGMT mRNA levels were assessed by qPCR. E. The same cells as in D were assessed for CAIX expression levels by qPCR. F. MGMT protein levels were assessed in LN-18, T98G or GS-2 M by immunoblot at 24 h or 48 h under hypoxic or normoxic conditions.

Supplementary Fig 3

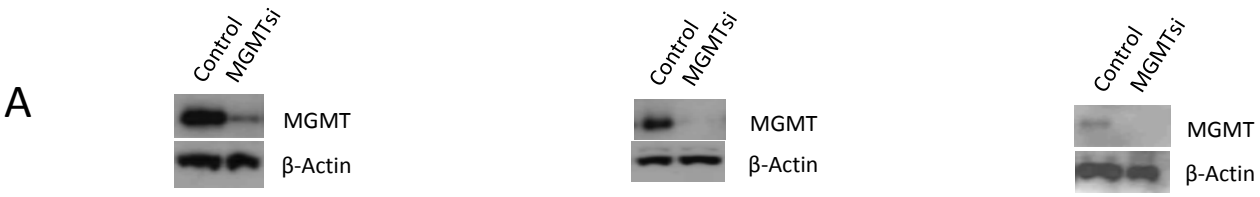

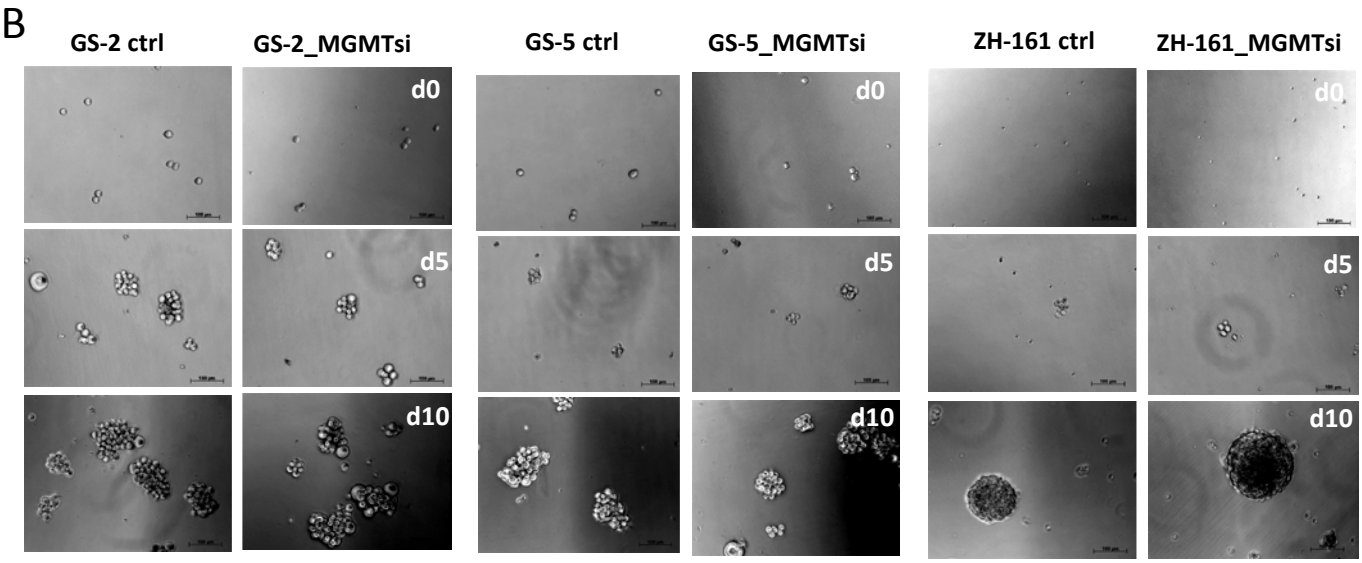

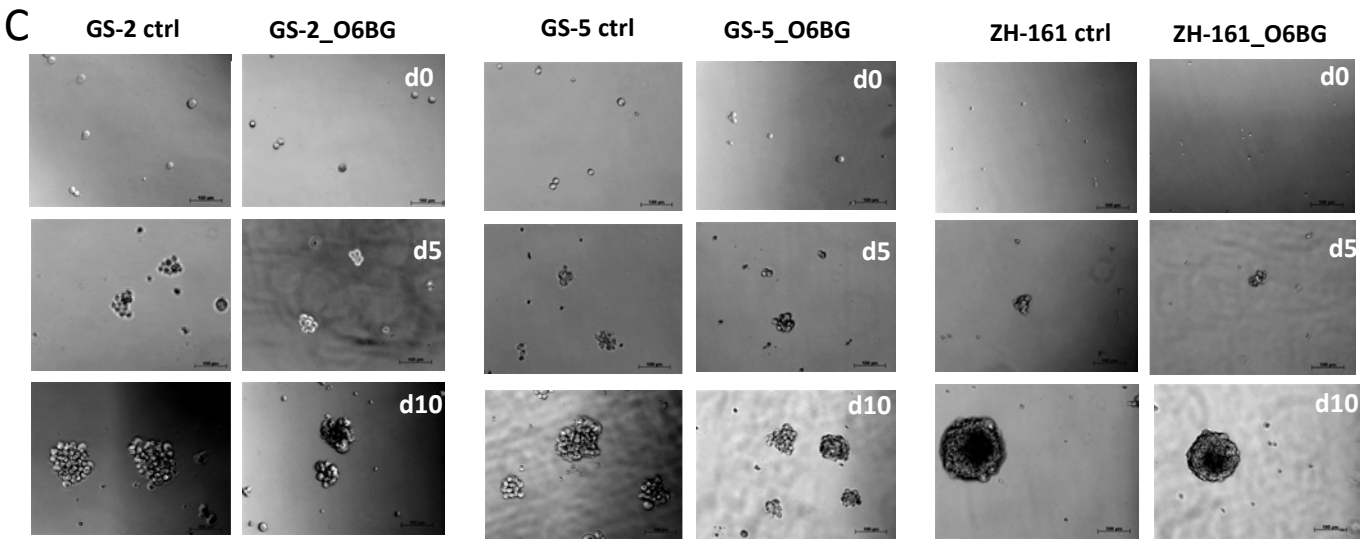

Supplementary Fig. 3. Sphere-formation capacity does not depend on MGMT expression. A. MGMT-expressing GS-2, GS-5 or ZH-161 S cells were transfected with MGMTsi or control. Down-regulation of MGMT protein was assessed by immunoblot. B. Sphere formation capacity was assessed and documented on days 5 and 10 (scale 100 μm). C. Sphere formation capacity was assessed in the same cells after exposure to O6-BG at the same time points (scale 100 μm).

Supplementary Fig 4

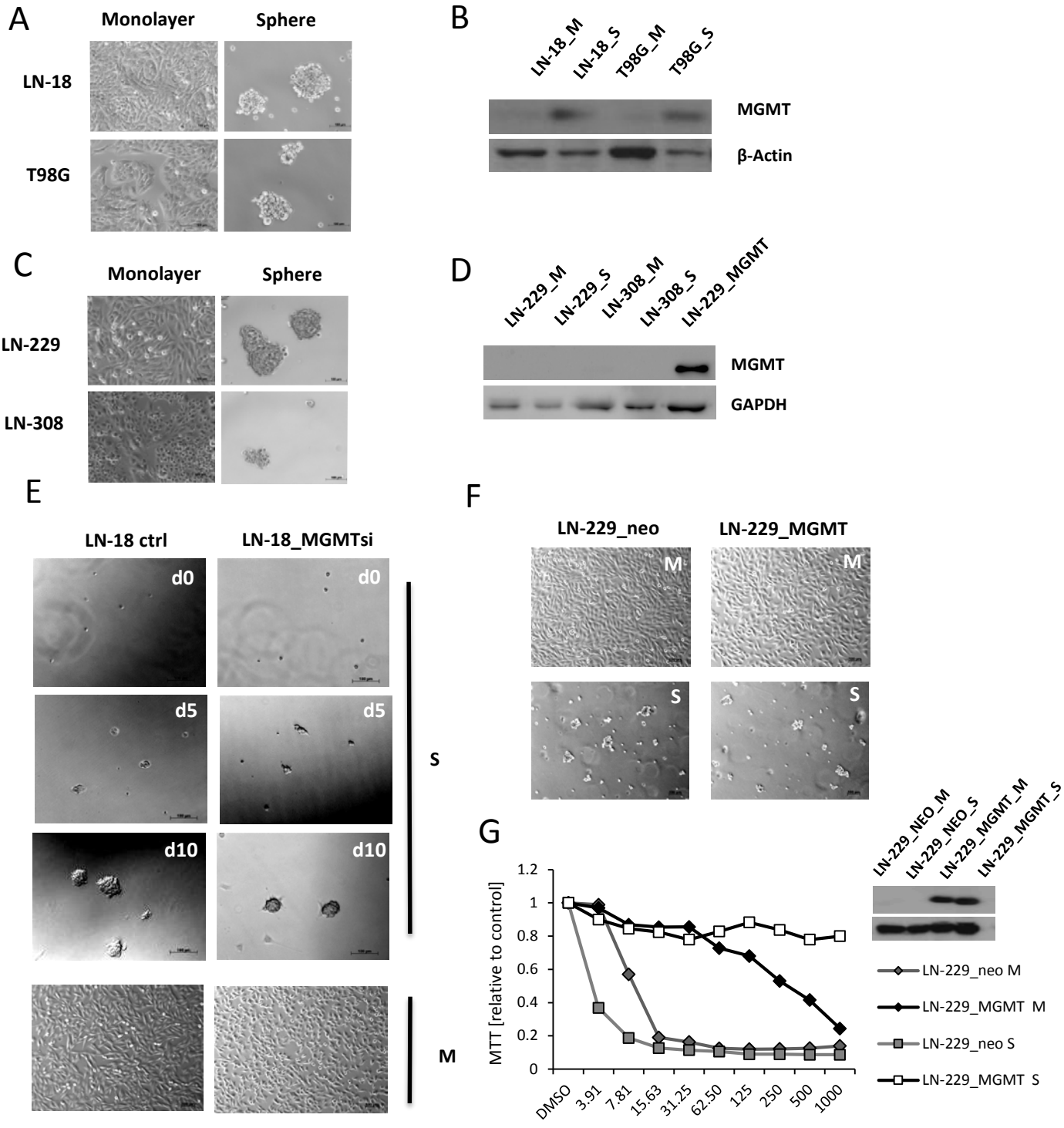

Supplementary Fig. 4. MGMT regulation in sphere-forming LTC. A. MGMT-expressing LN-18 or T98G cells were maintained under M or switched to S conditions to promote sphere formation (scale 100 µm). B. MGMT protein levels were assessed in the same cells by immunoblot. C, D. *MGMT* promoter-methylated LN-229 and LN-308 cells were studied as in A and B; LN-229_MGMT transfected cells were used as a positive control in D. E. LN-18 LTC cells expressing MGMT were transfected with MGMTsi or control. Sphere formation capacity was assessed and documented on days 5 and 10 (scale 100 µm). F. LN-229_MGMT transfected cells or LN-229_NEO control-transfected cells were maintained under M or switched to S conditions to promote sphere formation (scale 100 µm). G. The same cells were exposed to TMZ in indicated concentrations and clonogenic survival was assessed by MTT assay.